

## Competing electronic states under pressure in the double-exchange ferromagnetic Peierls system $\text{K}_2\text{Cr}_8\text{O}_{16}$

Touru Yamauchi,<sup>1,\*</sup> Kunihiro Hasegawa,<sup>1</sup> Hiroaki Ueda,<sup>2</sup> Masahiko Isobe,<sup>3</sup> and Yutaka Ueda<sup>4</sup>

<sup>1</sup>*Material Design and Characterization Laboratory, Institute for Solid State Physics, University of Tokyo, 5-1-5 Kashiwanoha, Kashiwa, Chiba 277-8581, Japan*

<sup>2</sup>*Solid State Physics and Chemistry Laboratory, Division of Chemistry, Graduate School of Science, Kyoto University, Kitashirakawa Oiwake, Sakyo-ku, Kyoto 606-8502, Japan*

<sup>3</sup>*Max Planck Institute for Solid State Research, Heisenbergstrasse 1, D-70569 Stuttgart, Germany*

<sup>4</sup>*Toyota Physical and Chemical Research Institute, 41-1 Yokomichi, Nagakute, Aichi 480-1192, Japan*

(Received 3 June 2014; revised manuscript received 8 February 2015; published 15 October 2015)

We investigated the pressure effect of  $\text{Cr}^{4+}/\text{Cr}^{3+}$  mixed-valence chromium oxide  $\text{K}_2\text{Cr}_8\text{O}_{16}$  using several kinds of high-pressure cells on the ferromagnetic Peierls transition. The resistivity measurements under pressure revealed that the Peierls phase ( $T_{\text{MI}} = 95$  K at 0 GPa) is suppressed but survives even at 13 GPa. Meanwhile, the ferromagnetic phase ( $T_{\text{C}} = 190$  K at 0 GPa) abruptly disappears at a relatively low pressure of 4 GPa. The two phase boundaries between metal/insulator (*non*-Peierls/Peierls) phases and between ferromagnetic/nonferromagnetic phases seem to cross each other, namely, the four phases seem to meet at a point in the pressure-temperature ( $P$ - $T$ ) phase diagram. At low temperature (Peierls insulating state), we also found an additional phase near the crossing point. These observations might realize the ground states theoretically predicted in the one-dimensional double-exchange system.

DOI: [10.1103/PhysRevB.92.165115](https://doi.org/10.1103/PhysRevB.92.165115)

PACS number(s): 71.30.+h, 74.62.Fj, 75.50.Dd

### I. INTRODUCTION

Material research is one of the key activities for modern physics as we have seen not only in high- $T_{\text{C}}$  cuprates, but also in many new compounds in which new interesting phenomena emerge.  $\text{K}_2\text{Cr}_8\text{O}_{16}$  is one such compound in which the recent theoretical and experimental works reveal the fascinating nature [1–5]. Because  $\text{Cr}^{6+}$  (no  $d$  electron) and  $\text{Cr}^{3+}$  (three  $d$  electrons,  $t_{2g}$  states half occupied) are considerably stable compared to other ionic states, there are a few compounds which take the  $\text{Cr}^{4+}$  and/or  $\text{Cr}^{5+}$  state. Despite such a situation, this compound actually takes a quite rare ionic state in the chemical point of view: the  $\text{Cr}^{4+}/\text{Cr}^{3+}$  mixed-valence state. In other words, four  $\text{Cr}^{4+}$  host ions in the  $\text{Cr}_4\text{O}_8$  framework share one additional electron that is doped by a guest cation  $\text{K}^+$ . Probably due to this ionic state, both the synthesis and the crystal growth of this compound require quite a high-pressure condition above 6 GPa. This experimental difficulty is one of the reasons why several decades have passed without any complementary report for physical properties such as the electric conduction and the magnetic susceptibility since the first discovery of this compound [6].

The “metal-to-insulator transition” (MIT) was first observed 33 years later [1] since the “discovery” of this compound [6] using *sub*-mm-size single crystals, that were grown by the  $\text{K}_2\text{Cr}_2\text{O}_7$  self-flux method (this also worked as an oxidation agent in high-pressure synthesis) under 6.7 GPa [1]. This MIT (the transition temperature,  $T_{\text{MI}} = 95$  K) was observed as a function of temperature in the resistivity measurements parallel to the  $c$  axis along which the crystal size was enough long to make the four electric contacts. Since the crystals had needlelike shape, the resistivity along other

directions has not been measured yet. As many literatures mentioned, the significance of this compound is that both phases above and below MIT ( $T_{\text{MI}} = 95$  K) are fully spin polarized ferromagnet [1–4,7,8]. Although there are many kinds of MITs as a function of temperature in the correlated electron systems including transition metal oxides (TMO), *no* MIT retaining the ferromagnetism has been observed in other compounds.

The first principle electronic structure calculations were carried out by Sakamaki *et al.* and they found the semimetallic/gapped majority/minority-spin bands structure responsible for the ferromagnetic and metallic nature above  $T_{\text{MI}}$  [2]. They also revealed that the conductive  $3d$ - $t_{2g}$  majority-spin band is composed of localized  $d_{xy}$  and itinerant  $d_{yz}$ ,  $d_{zx}$  bands responsible for the ferromagnetic nature generated by double-exchange (DE) mechanism, and pointed out that this situation is quite similar to that in the typical ferromagnetic metal compound  $\text{CrO}_2$  which has the localized  $d_{xy}$  and itinerant  $d_{yz\pm zx}$  bands structure [9]. Just after this calculation, the precise structure study by synchrotron x-ray diffraction measurements for the low-temperature insulating phase was performed [5]. Simultaneously, detailed electronic structure calculations using the obtained structure data were carried out [3]. The crystal structure of  $\text{K}_2\text{Cr}_8\text{O}_{16}$  can be divided into the host  $\text{Cr}_4\text{O}_8$  framework and the guest cation,  $\text{K}^+$  as shown in Fig. 1(a). The host  $\text{Cr}_4\text{O}_8$  framework represented by the network of blue  $\text{CrO}_6$  octahedra has two types of straight tunnels surrounded by double chains formed by edge-shared  $\text{CrO}_6$  octahedra running along the  $c$  axis. The  $\text{K}^+$  ions settle into the center of the larger tunnels. The calculations of Ref. [3] revealed that the stronger magnetic coupling between Cr ions does not sit at the Cr-Cr bondings within the double chain, but lies at those between the double chains via corner-shared oxygen atoms forming a smaller rutilelike tunnel (no  $\text{K}^+$  in it) as shown in Fig. 1(b). This is due to the strong admixture

\*yamauchi@issp.u-tokyo.ac.jp

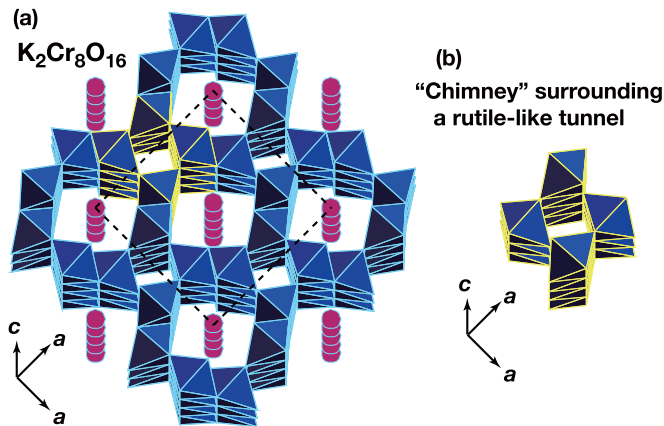


FIG. 1. (Color online) Tetragonal crystal structure of  $\text{K}_2\text{Cr}_8\text{O}_{16}$ . (a)  $\text{Cr}_4\text{O}_8$  framework formed by  $\text{CrO}_6$  octahedra (blue) and K ions (red balls), and (b) "chimney" structure formed by corner-shared  $\text{CrO}_6$  octahedra in the  $\text{Cr}_4\text{O}_8$  framework.

of Cr  $d_{yz\pm zx}$  and corner-shared O  $p_z$  bands at the Fermi level. Therefore, the quasi-one-dimensional (q1D) electron system unexpectedly sits on the "chimney" formed by corner-shared  $\text{CrO}_6$  octahedra around the rutilelike tunnels rather than the edge-shared double chains which are naively supposed to be an origin of q1D nature.

The problem is how the  $\text{K}^+$ -doped electrons in the q1D "chimney" behave at the MIT. The precise crystal structure analysis in the insulating phase reveals almost no charge disproportionation (less than 0.03 electron) among the Cr sites. The calculated Fermi surface of the ferromagnetic metal phase has a strong nesting wave vector  $Q_z = 2\pi/c$  that also agrees with the observed superstructure ( $\sqrt{2} \times \sqrt{2} \times 1$ ) in the insulating phase. Therefore, these experimental and theoretical results strongly support the following scenario; This MIT results from the Peierls mechanism and a localized  $\text{K}^+$ -doped electron is shared by the four Cr ions [3]. This situation is probably responsible for the DE mechanism in the Peierls gap opening insulator state. Actually, there is one theoretical study approaching this situation [4], in which the DMRG calculation on the 1D-DE model at quarter filling with lattice dimerization reveals three kinds of ground states: ferromagnetic insulating state FI ( $S = S_{\max}$ ) with Peierls gap and full spin polarization  $S_{\max}$ , paramagnetic insulating state PI ( $S = 0$ ) with Mott gap and dominant antiferromagnetic spin correlation, and intermediate state FI ( $0 < S < S_{\max}$ ) with the partial spin polarization between the FI and PI states. These three ground states contact each other in the parameter space expanded by  $J_H/t$  and  $\delta$ , where  $J_H$ ,  $t$ , and  $\delta$  are the Hund's coupling energy, conduction band width, and Peierls gap, respectively (see Fig. 2 in Ref. [4]). Note that these phases are implied to have the characteristic spin structures, what we called "island" and "spiral"-type structures, and have been argued in the long history of the studies in metallic DE systems [10].

In this work, we present a pressure-temperature ( $P$ - $T$ ) phase diagram of  $\text{K}_2\text{Cr}_8\text{O}_{16}$ , that is a good system to cast a light on the 1D-DE system with Peierls gap. We will show the several ground states near and beyond the pressure where the multicritical point (MCP) appears. The theoretical

prediction seems to well explain our observations including an intermediate ferromagnetic insulating (iFI) phase.

## II. EXPERIMENTALS

A multianvil-type high-pressure cell equipped with sintered diamond anvils was employed for the resistivity measurements along the  $c$  axis up to 13 GPa, and a piston cylinder-type high-pressure cell equipped in the PPMS (Quantum Design) was employed to measure the transverse magnetoresistance along the  $c$  axis up to 3 GPa. The magnetic properties up to 4 GPa were observed with a miniature ceramic-anvil high-pressure cell which was recently designed to be equipped in the MPMS (Quantum Design) [11]. Both resistivity and magnetoresistance measurements were performed using single crystals with the excitation current along the q1D "chimney" direction (the magnetic field  $H$  was applied perpendicular to the "chimney"). Meanwhile, the magnetic measurements were carried out with the polycrystalline sample because the volume of the crystals was too small to generate a large enough signal in the high background signal resulting from the pressure cell, which was subtracted numerically from the raw signal.

## III. RESULTS

### A. The resistivity under pressure

Two sets of resistivity-temperature ( $\rho$ - $T$ ) curves observed up to 13 GPa are exhibited in Fig. 2. One set of  $\rho$ - $T$  curves was obtained with a multianvil-type cell (3.5–13 GPa) and the other was obtained with a piston cylinder-type cell (0–2.7 GPa). Some gap between these two sets of  $\rho$ - $T$  curves is probably due to the error in measuring the sample crystal dimension. This figure clearly shows the robust insulating nature against the pressure even at 13 GPa. One can find the Peierls phase

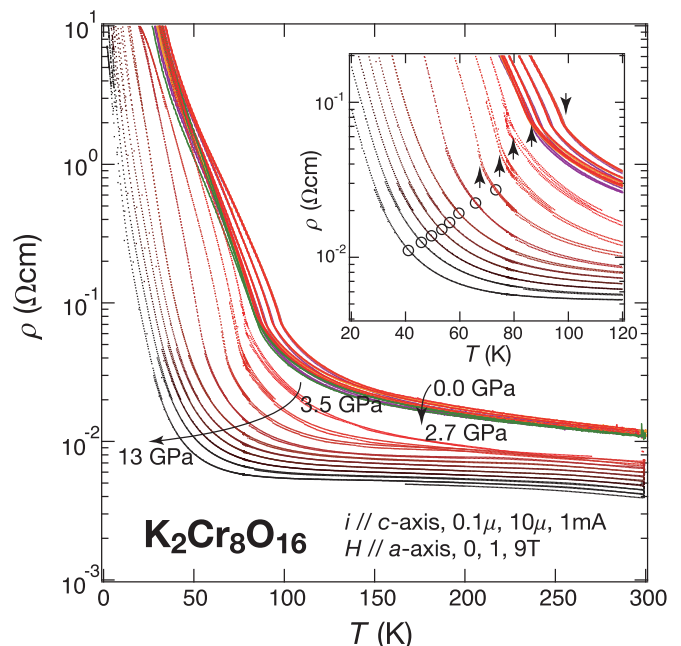


FIG. 2. (Color online) A set of the resistivity-temperature ( $\rho$ - $T$ ) curves up to 13 GPa. The inset is the macrograph to show the pressure evolution of the Peierls transition.

survives at least up to about 5 GPa where each  $\rho$ - $T$  curve has a bending point as shown by a small arrow in the inset of Fig. 2. The transition temperature  $T_{MI}$  is about 70 K at 5 GPa. It is natural that the anomaly (bending point) on the  $\rho$ - $T$  curve under pressure represents the Peierls transition as observed in the  $\rho$ - $T$  curve at ambient pressure. Above 5 GPa, the clear bending point disappears and the  $\rho$ - $T$  curves show round upturn with decreasing temperature as observed in narrow-gap semiconductors. Here we define the expedient  $T_{MI}$  as a peak of  $d^2(\log\rho)/dT^2$  above 5 GPa. This is depicted by small open circles in this figure, which will appear in a later section. It is noteworthy that  $K_2Cr_8O_{16}$  has a 1D-like electronic state even under the highest pressure, because the Peierls instability which is one characteristic of the 1D system still remains at 13 GPa.

### B. The magnetization under pressure

Next, we focus on the magnetic properties under pressure up to 4.1 GPa. Figure 3(a) exhibits the pressure evolution of the magnetization-temperature ( $M$ - $T$ ) curves observed at two different external magnetic fields, 0.1 and 5 T. Figure 3(b) shows magnetization-magnetic field ( $M$ - $H$ ) curves at 2, 80, 150, and 250 K up to 7 T under various pressures. These figures evidently display the considerably gracile ferromagnetic nature against pressure. The Curie temperature ( $T_C$ ) was

determined from the  $M$ - $T$  curves at 0.1 T as shown by the red cross (color online) in Fig. 3(a). At 1.1 GPa,  $T_C$  decreases by about 30 K while keeping the shape of the  $M$ - $T$  curve of 0.1 T. At 2.3 GPa, the ferromagnetic nature still remains but the ferromagnetic shape of the curve seems to collapse in the wide temperature region below  $T_C$ . At 4.1 GPa, there is no sign of ferromagnetism on the  $M$ - $T$  curve of 0.1 T. In contrast, the  $M$ - $T$  curves at 5 T show the ferromagnetic behavior up to 3.2 GPa. Note that the ferromagnetism is assisted by magnetic field and suppressed by pressure in this system. This situation is also observed in the pressure evolution of  $M$ - $H$  curves. The steep rising of low-temperature  $M$ - $H$  curve characteristics of ferromagnetism can be seen below 2.3 GPa, while above 2.3 GPa, the slope of the  $M$ - $H$  curve at 2 K begins to sharply decrease with increasing pressure. As a result, the saturation field ( $H_s$ ) depicted by a black circle in Fig. 3(b) increases with increasing pressure above 2.3 GPa. Here,  $H_s$  is defined as the field where the  $d^2M(2K)/dH^2$  curve has a peak and is not that where the  $M$  reaches the fully polarized moment,  $M_{full}$ , or the saturation. Furthermore, we emphasize that the saturated magnetization  $M_s$  seems to decrease meaningfully above 2.3 GPa. These results of magnetic properties suggest the existence of an intermediate ferromagnetic (iFI) phase between ferromagnetic (below 2.3 GPa) and nonferromagnetic (above 4.1 GPa) insulating phases.

### C. The magnetoresistance under pressure

The existence of the iFI phase was also observed in magnetoresistance (MR) measurements. It is natural to suppose that the iFI phase affects the electromagnetic properties of this system. We indeed discovered a characteristic phenomena in the iFI phase. The pressure evolution of the MR curves [ $\rho(H)/\rho(0)$  as a function of temperature] measured at  $H = 1$  and 9 T is exhibited in Fig. 4. The MR curves at 0 GPa well reproduce the previous observation [1] and one can see both  $T_{MI}$  and  $T_C$  as shown in Fig. 4 by the symbols of blue triangle and red cross (filled, 1 T; open, 9 T), respectively. Strictly, this  $T_C$  is lower than that derived from the  $M$ - $T$  curve, because a dimple on the MR curve corresponds to a peak on the  $dM/dT$  curve. Note that  $T_{MI}$  does not change and  $T_C$  becomes about 10 K higher by applying the magnetic field of 9 T (see both MR curves at 1 and 9 T in 0.0 and 0.9 GPa). It is feasible that the magnetic field does not affect Peierls transition but assists the ferromagnetic transition. As increasing pressure  $T_C$  approaches to  $T_{MI}$  and the two merge at about 2.0 GPa. In the pressure region below 2.0 GPa, where  $M_s = M_{full}$  at 2 K, the MR is approximately 90% at the minimum in both the FI and FM phases. Above 2.2 GPa, where  $M_s < M_{full}$ , both MR curves below  $T_{MI}$  at 1 and 9 T suddenly show a large drop down to 70%. At 2.5 GPa, these MR at low temperature decrease to about 50%. At 2.7 GPa, the MR of 1 T becomes close again to the unity, but that of 9 T is still far from the unity. This observation also gives us another evidence for the appearance of the iFI phase at around 2.5 GPa. Especially, the optimum feature of MR of 1 T at 2.5 GPa is meaningful when we discuss the  $P$ - $T$  phase diagram of this compound. A significant difference between MR of 1 T and 9 T at 2.7 GPa can be attributed to a difference of the  $P$ - $T$  phase diagrams under 1 T and 9 T. It is reasonable

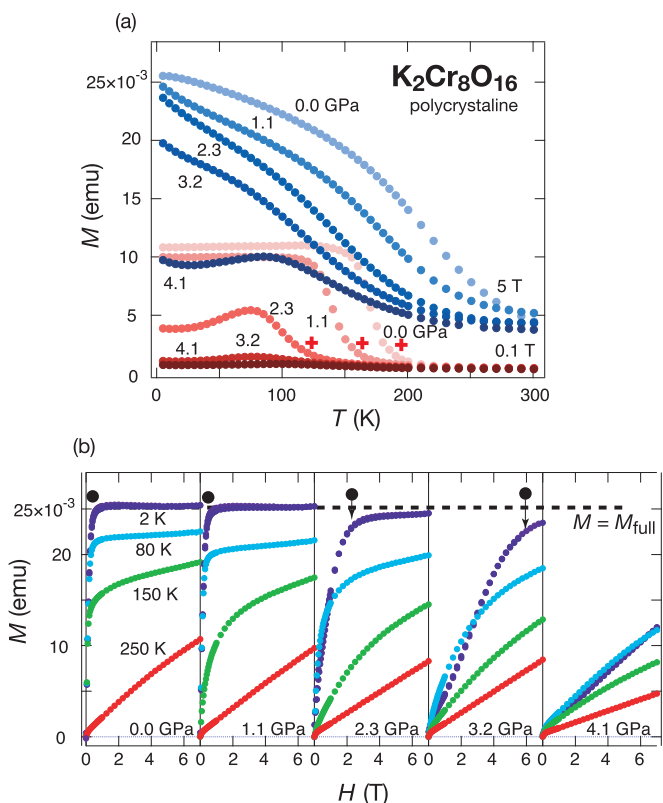


FIG. 3. (Color online) The magnetization under pressure up to 4.1 GPa. (a) Temperature dependence ( $M$ - $T$  curves) at 0.1 T (red) and 5 T (blue), and (b) magnetic field dependence ( $M$ - $H$  curves) at 2, 80, 150, and 250 K up to 7 T. The red cross on the  $M$ - $T$  curves of 0.1 T shows Curie temperature  $T_C$ , and the black circle on the  $M$ - $H$  curves of 2 K shows saturation field  $H_s$ .

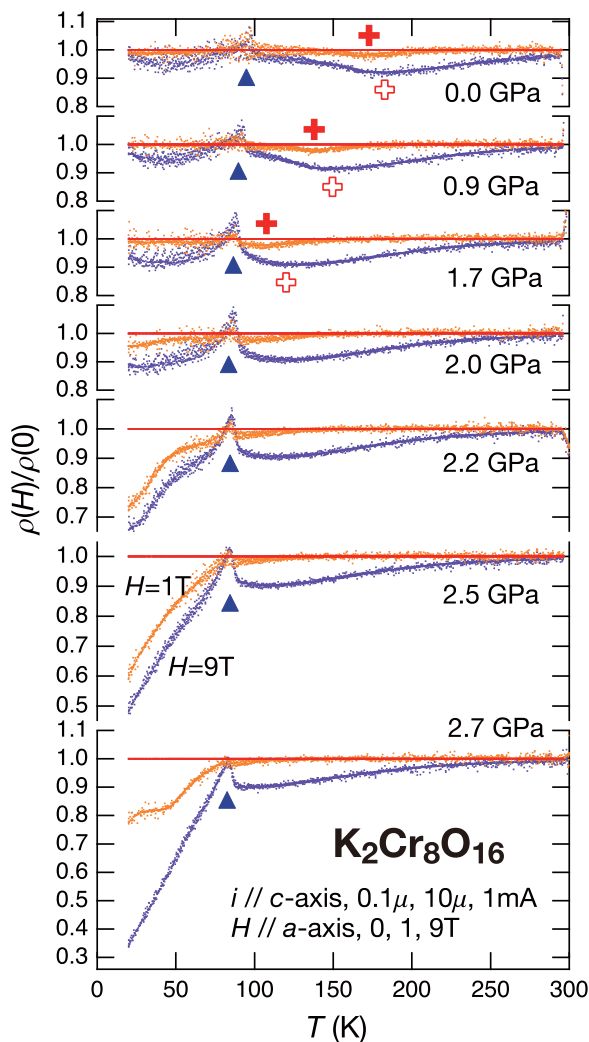


FIG. 4. (Color online) The magnetoresistance (MR) curves under several pressures up to 2.7 GPa: The ratio of the resistivity at  $H = 1$  (orange line) and 9 T (blue line) to that at zero field. Relatively large negative magnetoresistance (over 30%) suddenly appears below  $T_{MI}$  at around 2.2 GPa.

to suppose phase boundary shifting toward the higher pressure region under higher magnetic field, because the high magnetic field can stabilize the phase that has large magnetic moment such as FI and/or iFI phases. Furthermore, it is noteworthy that large MR probably characteristic of the iFI phase could be observed only within the narrow  $P$ - $T$ - $H$  region near the phase boundary included in the FI phase (see the Fig. 2 in Ref. [4]).

#### D. The phase diagram

To summarize our observations, the  $P$ - $T$  and the pressure-field ( $P$ - $H$ ) phase diagrams are represented in Fig. 5. The main panel and the inset show  $P$ - $T$  and  $P$ - $H$  diagrams, respectively. The symbols of both the blue filled triangle and the blue open circle represent  $T_{MI}$ s derived from the bending point of  $\rho$ - $T$  curves and the peak point of  $d^2(\log\rho)/dT^2$ , respectively. The green area denotes the insulating phase which is robust against pressure. Meanwhile, the symbol of the red cross shows  $T_C$

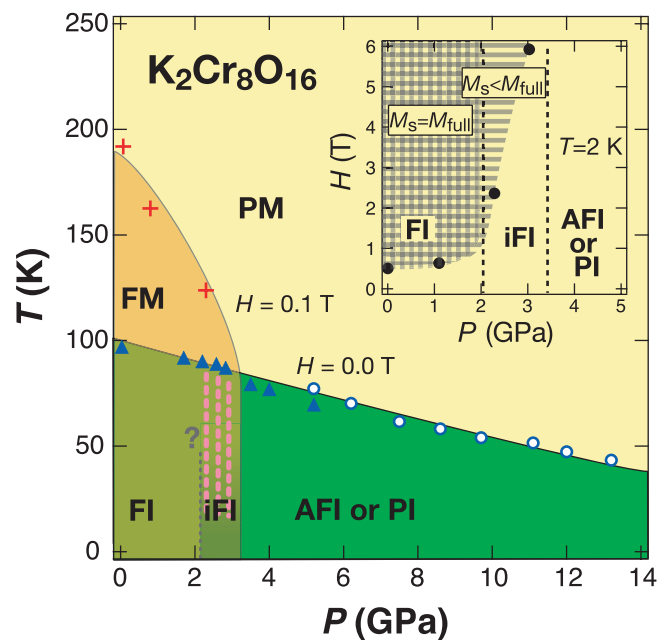


FIG. 5. (Color online) The  $P$ - $T$  phase diagram. The crossing of the phase boundaries (M/I and F/non-F) results in four main phases, FM, PM, FI, and AFI or PI (see text). iFI phase seems to appear between FI and AFI/PI phases. The  $P$ - $T$  region where the large MR is observed is also depicted by the red bold broken line. The inset shows the pressure dependence of  $H_s$  [filled circles marked on  $M$ - $H$  curves in Fig. 3(b)]. This corresponds to the  $P$ - $H$  phase diagram at 2 K that depicts three regions as explained in the text.

estimated from the  $M$ - $T$  curves at 0.1 T. The orange area means the ferromagnetic phase that is gracile against pressure. This  $P$ - $T$  phase diagram, thus, consists of four main phases; ferromagnetic metal (FM), paramagnetic metal (PM), ferromagnetic insulator (FI), and antiferromagnetic or paramagnetic insulator (AFI/PI). The most significant aspect of this diagram is a crossing of two phase boundaries. The boundary between metal and insulator seems to lie across the boundary between ferromagnet and paramagnet (or antiferromagnet) without any interference. Therefore, the main four phases meet at a point in the  $P$ - $T$  plane, that is called the “multicritical point” (MCP).

In addition to the main four phases, an intermediate ferromagnetic insulator (iFI) phase seems to lie near the MCP. The inset of Fig. 5 shows the pressure dependence of  $H_s$  from which the three phases characteristic of  $M_s = M_{full}$  (FI),  $M_s < M_{full}$  (iFI), and no ferromagnetic sign on the  $M$ - $T$  (0.1 T) curve (AFI/PI) can be deduced. These three areas at 2 K are interpreted as three kinds of magnetic ground states accompanied by the considerable pressure evolution of  $H_s$ . The boundaries between FI and iFI and between iFI and AFI/PI are roughly figured out by taking the results of both magnetization and the magnetoresistance measurements into account. In the main panel of Fig. 5, the  $P$ - $T$  region where the large MR was observed is illustrated by bold red vertical broken lines. The precise phase boundary between iFI and FI phases at finite temperature is still unclear; however, it is tentatively drawn by a vertical broken line in this diagram because the large MR suddenly appears just below  $T_{MI}$ . It is noteworthy

that the optimum feature of MR at 1 T under 2.5 GPa and the shape of  $M$ - $H$  curves under 2.3 and 3.2 GPa are good evidences for the iFI phase that emerges between FI and AFI/PI phases.

#### IV. DISCUSSION

The present study has revealed some important pressure effects on the ferromagnetic MIT of the DE ferromagnetic Peierls system  $K_2Cr_8O_{16}$ .

- (1) The FM phase, i.e.,  $T_C$  is suppressed very rapidly.
- (2) The MIT is considerably robust.
- (3) The ferromagnetism disappears at the critical point where  $T_C$  meets  $T_{MI}$ , leading to the transition from the PM phase to the AFI/PI phase by lowering temperature, and the four phases, PM, FM, FI, and AFI/PI seem to meet at a multicritical point (MCP).
- (4) The intermediate ferromagnetic insulator (iFI) phase exists between FI and AFI/PI.

The first point (i) agrees with the fact that  $Rb_2Cr_8O_{16}$  with larger unit cell volume (negative pressure) has a higher  $T_C = 295$  K [12]. In contrast to these Cr hollandites, the ferromagnetism in another DE ferromagnetic metal system  $CrO_2$  with a similar “chimney” structure but without large tunnels which accommodate K (Rb) ions is quite robust against high pressure and is expected to vanish under approximately 60 GPa accompanied by a half-metal-to-metal transition [13,14]. Therefore such a substantial pressure dependence of  $T_C$  in Cr hollandites could be attributed to the existence of large tunnels in the hollandite structure.

In DE ferromagnetic systems, the ferromagnetism originates from the Hund’s rule coupling  $J_H$  and is governed by kinetics of itinerant electrons, i.e., the hopping parameter  $t$ . Since  $J_H$  is considered to be insensitive to pressure, the pressure dependence of  $T_C$  may be attributed to the pressure dependence of  $t$ . It is natural that the applying pressure makes  $t$  increase, because the atomic distance is shortened by pressure. Why is the pressure dependence of  $T_C$  so different between Cr hollandites and  $CrO_2$ ? In  $CrO_2$  a “chimney” formed by four edge-shared  $CrO_6$  chains shares the chains with the neighboring “chimney,” while in Cr hollandite it does not share them but is linked via double chains to others (see Fig. 1). This crystallographic difference probably accounts for both 3D-like natures in  $CrO_2$  and rather 1D-like natures in Cr hollandites. In general, it has been empirically known that the electronic states of 3D-like TMO are robust against pressure up to several dozen GPa. In contrast, the electronic states of 1D-like TMO are substantially affected by pressure. Therefore, the observed steep suppression of FM, i.e.,  $T_C$  could be due to the increase of  $t$  under pressure.

The second point (ii), on the other hand, is just how it is expected, because the MIT is a second-order transition without volume change at the transition. Such an insensitive pressure dependence of  $T_{MI}$  suggests that the lattice deformation (dimerization) in the Peierls state is rather stiff. As a result, this robust MIT leads to a very rich  $P$ - $T$  phase diagram as described in the pressure effects and enables us to compare the obtained phase diagram with the theoretical prediction [4].

There exists the general relation between magnetism and electronic transport properties that insulating TMOs are typically antiferromagnetic, and ferromagnetism, particularly DE ferromagnetism, goes hand in hand with metallicity. In this close relation between ferromagnetism and metallicity, the FI ground state resulting from the Peierls-type MIT in the DE-ferromagnetic system is quite uncommon. Nishimoto and Ohta studied the effects of opening the band gap in a 1D DE-ferromagnetic system, with  $K_2Cr_8O_{16}$  in mind, by applying the numerical density-matrix renormalization group (DMRG) technique [4]. They found that the metallicity itself is not a necessary condition for the realization of the DE ferromagnetism and presented the ground-state phase diagram in the parameter space expanded by the Hund’s coupling constant divided by hopping parameter  $J_H/t$ , and the dimerization strength  $\delta$  ( $0 < \delta \leq 2$ ). Their calculations yielded that there are three kinds of ground states, FI ( $S = S_{max}$ ), FI ( $0 < S < S_{max}$ ), and PI ( $S = 0$ ), depending on the values of  $J_H/t$  and  $\delta$ , where  $S_{max}$  denotes the full spin polarization. The FI ( $S = S_{max}$ ) state appears when  $J_H/t$  is large, the PI ( $S = 0$ ) state appears when  $J_H/t$  is small, and in between, the FI ( $0 < S < S_{max}$ ) state with the intermediate spin polarization also appears. The FI phase in the present study has full magnetization, while the iFI phase has meaningfully somewhat smaller magnetization and the AFI/PI phase shows no ferromagnetism. These experimental results indicate that our observed FI ( $M_s = M_{full}$ ), iFI ( $M_s < M_{full}$ ), and AFI/PI phases well coincide with the theoretically obtained FI ( $S = S_{max}$ ), FI ( $0 < S < S_{max}$ ), and PI ( $S = 0$ ) states, respectively. Furthermore the Nishimoto-Ohta phase diagram predicts the successive ground-state change as FI ( $S = S_{max}$ )  $\rightarrow$  FI ( $0 < S < S_{max}$ )  $\rightarrow$  PI ( $S = 0$ ) when  $J_H/t$  decreases at constant  $\delta$  ( $0 < \delta < 2$ ). Since the increasing pressure makes  $t$  ( $J_H/t$ ) increase (decrease), as already discussed with the first pressure effect (i), and  $\delta$  is insensitive to the pressure (the insulating Peierls state is robust), the observed ground-state change, FI  $\rightarrow$  iFI  $\rightarrow$  AFI/PI with increasing pressure can be well explained as the ground-state change, FI ( $S = S_{max}$ )  $\rightarrow$  FI ( $0 < S < S_{max}$ )  $\rightarrow$  PI ( $S = 0$ ) with decreasing  $J_H/t$  at constant  $\delta$  ( $0 < \delta < 2$ ) in the Nishimoto-Ohta phase diagram.

Next we would like to discuss the spin states of the iFI and AFI/PI phases. Nishimoto and Ohta suggested that the FI ( $0 < S < S_{max}$ ) state may be similar to the “spiral”-type spin state in 1D Kondo and Hund lattices [10] or the incommensurate (IC) state in manganites [15–17], meanwhile the PI ( $S = 0$ ) state may be similar to the “island”-type spin state in 1D Kondo and Hund lattices [10], although both “spiral”- and “island”-type spin states are obtained from the calculations at  $\delta = 0$  (metal region) in contrast to the present case at  $0 < \delta \leq 2$  (insulator region). Then the iFI and AFI/PI phases may have “spiral”- and “island”-type spin states, respectively. The difference between “spiral”- and “island”-type spin states is in  $q$ -vector dependence of the spin structure factor  $S(q)$ . The  $S(q)$  of the “island”-type spin state has a peak at  $q = 2k_F = \pi/n$ , ( $1/n$ , carrier density per site in the 1D DE system). Namely, zero total spin number in a 1D DE system,  $s_{tot} = 0$ , is expected in some spin arrangement, i.e., “ $\uparrow\uparrow\downarrow\downarrow\uparrow\uparrow\downarrow\downarrow$ ”. In another case such as “ $\uparrow\uparrow\uparrow\downarrow\downarrow\uparrow\uparrow\downarrow\downarrow$ ”, a fractional total spin number,  $0 \leq s_{tot} < s_{full}$ , is expected. Note that the above two kinds of spin states have commensurate

spin configurations in a 1D spin system. Meanwhile, the  $S(q)$  of the “spiral”-type spin state has a peak at  $0 < q < \pi/n$ , which shows an incommensurate spin structure in the 1D system. Note that this incommensurate state smoothly connects with the FM ( $q = 0$ ) and the “island”-type ( $q = \pi/n$ ) states. Both “island”- and “spiral”-types are quite peculiar spin states characteristic of 1D systems in which the interaction between conduction electrons and quantum localized spins is essential.

These “island”- and “spiral”-type spin states favorably explain our observations in the magnetization and the magnetoresistance measurements under pressure. As already discussed in previous sections, the nonferromagnetic character in AFI/PI phases can be explained by “island”-type spin state, in which a smaller or zero total spin moment in the 1D DE system is expected. A characteristic magnetic behavior in the iFI phase, such as  $M_s < M_{\text{full}}$ , can also be explained by the “spiral”-type spin state. Furthermore, the peculiar behaviors of MR can be explained by the “island”- and “spiral”-type spin structures in the 1D “chimney” system (we observed the conduction along the “chimney”  $c$  axis). The relatively large MR in a typical DE compound,  $\text{La}_{1-x}\text{Sr}_x\text{MnO}_3$  ( $x \sim 0.17$ ), is observed at around the paramagnetic insulator phase just above the low-temperature ferromagnetic metal phase [18]. This is explained as follows: The hopping probability of electrons in the  $e_g$  band that are Hund coupled with the localized  $t_{2g}$  spins is sensitive to an external magnetic field ( $H_{\text{ex}}$ ) in a paramagnetic phase, because the canting angle between the neighboring two  $t_{2g}$  spins is easily decreased in the paramagnetic phase and is hard to change in the ferromagnetic phase by applying  $H_{\text{ex}}$ . Moreover, small MR in the metallic phase compared with that in the insulating phase is probably caused by the different conduction processes of Bloch electrons (metallic phase) from that of further localized electrons (insulating phase).

In  $\text{K}_2\text{Cr}_8\text{O}_{16}$ , the “spiral”-type spin state for the iFI phase would have a  $t_{2g}$  spin structure modulated in an incommensurate manner. Namely, a spin structure factor  $S(q)$  has a peak at  $q \neq 0$  and this peak can shift continuously in  $q$  space. This manner of spin structure can be expected to allow an  $H_{\text{ex}}$ -sensitive configuration between the neighboring two  $t_{2g}$  spins in the “chimney” system. This possibly causes large MR in the iFI phase. Meanwhile, the  $t_{2g}$  spins are considered to align completely and alternatively in some commensurate manners in the FI and AFI/PI phases, respectively. In these cases, a  $S(q)$  peak (at  $q = 0$  in FI or at  $q = m/n$  in AFI/PI) can move only discretely. This situation is applicable to  $H_{\text{ex}}$ -insensitive conduction. Therefore, FI  $\rightarrow$  iFI (“spiral”-type)  $\rightarrow$  AFI/PI (“island”-type) successive transition at low temperature seems to explain an optimum feature of MR at 1 T.

Apart from the comparison with the theoretical predictions, one may simply consider the iFI phase as a coexistence of the FI and AFI/PI phases, because coexistence behaviors of two electronic phases have been often observed around the critical point in the  $P$ - $T$  electronic phase diagram [19]. The coexistence of FI and AFI/PI phases may be responsible for the peculiar electromagnetic features observed in the iFI area,  $M_s < M_{\text{full}}$ , and the large MR. However, a macroscopic coexistence, in which a typical size of the grain ( $\xi$ ) is far larger than the lattice space ( $a$ ), is unlikely. If the iFI phase were such

a phase with macroscopic FI phase grains, the  $M$ - $H$  curves would show the saturation behavior at around 0.5 T even under pressures like the pure FI phase [see Fig. 3(b) of 1.1 GPa]. In reality the  $M$ - $H$  curves of the iFI phase above 2.3 GPa show the saturation in considerably high magnetic fields. Meanwhile, a microscopic coexistence, in which  $\xi$  is the same order of magnitude as  $a$ , may be feasible. The  $S(q)$  in such a microscopic coexistence state would have many and/or broad peaks at  $0 < q < m/n$ . Namely its  $t_{2g}$  spin structure seems to take a modulated spin structure with a dis-commensurate manner in the “chimney” system, which would be responsible for the peculiar electromagnetic properties mentioned above.

Incidentally, such coexistence of electronic states at around the critical point has been believed to be caused by the competition and/or fluctuation of various interactions. The theoretical intermediate state, FI ( $0 < S < S_{\text{max}}$ ) in the Nishimoto-Ohta phase diagram would result from the competition and/or fluctuation of the interactions:  $J_{\text{H}}$ ,  $t$ , and  $\delta$ . It is an intriguing question to figure out what causes the difference between phase coexistence and the homogenous intermediate phase at the critical pressure in the phenomenological sense. We have no data to distinguish between the two at present. Therefore, further experimental and theoretical studies are desirable so that we can know the microscopic spin states under pressure, although some experimental difficulties in high-pressure experiments and in crystal growth of  $\text{K}_2\text{Cr}_8\text{O}_{16}$  prevent us from probing such microscopic features.

Finally we would like to emphasize that  $\text{K}_2\text{Cr}_8\text{O}_{16}$  is really a 1D DE ferromagnetic Peierls system which is very rare as a real material and therefore is very worthy in the sense that it enables one to verify theoretical predictions. As a result, the present study seems to show the realization of the theoretical prediction although the pure 1D DE model may not be sufficient for quantitative discussions on the real material.

## V. CONCLUSION

In this work, we first performed the high-pressure study (resistivity, magnetization, and magnetoresistance measurements) in the DE ferromagnetic Peierls system  $\text{K}_2\text{Cr}_8\text{O}_{16}$ , and we established the  $P$ - $T$  electronic phase diagram. The FM phase is suppressed very rapidly, while the MIT (Peierls state) is considerably robust. As a result,  $T_{\text{C}}$  meets  $T_{\text{MI}}$  at the critical point where the ferromagnetism disappears, leading to the transition from the PM phase to the AFI/PI phase by lowering temperature, namely the four phases, PM, FM, FI, and AFI/PI, meet at the MCP. Furthermore, we discovered some possible signs for an appearance of the iFI phase, which was characterized by the fairly reduced magnetic moment from the fully polarized moment and the significantly large negative MR, between FI and AFI/PI. The observed ground states, FI ( $M_s = M_{\text{full}}$ ), iFI ( $M_s < M_{\text{full}}$ ), and AFI/PI, seem to well coincide with the theoretically predicted ground states, FI ( $S = S_{\text{max}}$ ), FI ( $0 < S < S_{\text{max}}$ ), and PI ( $S = 0$ ). The iFI phase possibly has the spin state similar to the “spiral”-type in 1D Kondo and Hund lattices or may be a microscopic coexistence of FI and AFI/PI phases. The observed ground-state change, FI  $\rightarrow$  iFI  $\rightarrow$  AFI/PI, as a function of pressure seems to well

realize the ground-state change along the decreasing  $J_H/t$  at constant  $\delta$  in the calculated ground-state phase diagram of the 1D DE model at a quarter filling with the lattice dimerization, indicating that the pressure mainly makes it increase. These results tell us again that  $K_2Cr_8O_{16}$  is a typical but very rare example of the 1D DE ferromagnetic Peierls system.

### ACKNOWLEDGMENTS

The authors thank Prof. Y. Ohta, Prof. H. Nakao, for fruitful discussions. T.Y. also thanks Dr. N. Tateiwa for some instructions on the miniature ceramic-anvil high-pressure cell. This study is supported by a Grant-in-Aid for Scientific Research (No. 22244041) from the Japan Society for the Promotion of Science.

- 
- [1] K. Hasegawa, M. Isobe, T. Yamauchi, H. Ueda, J.-I. Yamaura, H. Gotou, T. Yagi, H. Sato, and Y. Ueda, *Phys. Rev. Lett.* **103**, 146403 (2009).
  - [2] M. Sakamaki, T. Konishi, and Y. Ohta, *Phys. Rev. B* **80**, 024416 (2009).
  - [3] T. Toriyama, A. Nakao, Y. Yamaki, H. Nakao, Y. Murakami, K. Hasegawa, M. Isobe, Y. Ueda, A. V. Ushakov, D. I. Khomskii, S. V. Streltsov, T. Konishi, and Y. Ohta, *Phys. Rev. Lett.* **107**, 266402 (2011).
  - [4] S. Nishimoto and Y. Ohta, *Phys. Rev. Lett.* **109**, 076401 (2012).
  - [5] A. Nakao, Y. Yamaki, H. Nakao, Y. Murakami, K. Hasegawa, M. Isobe, and Y. Ueda, *J. Phys. Soc. Jpn.* **81**, 054710 (2012).
  - [6] T. Endo, S. Kume, N. Kinomura, and M. Koizum, *Mater. Res. Bull.* **11**, 609 (1976).
  - [7] P. Mahadevan, A. Kumar, D. Choudhury, and D. D. Sarma, *Phys. Rev. Lett.* **104**, 256401 (2010).
  - [8] H. Takeda, Y. Shimizu, M. Itoh, M. Isobe, and Y. Ueda, *Phys. Rev. B* **88**, 165107 (2013).
  - [9] M. A. Korotin, V. I. Anisimov, D. I. Khomskii, and G. A. Sawatzky, *Phys. Rev. Lett.* **80**, 4305 (1998).
  - [10] D. J. Garcia, K. Hallberg, B. Alascio, and M. Avignon, *Phys. Rev. Lett.* **93**, 177204 (2004).
  - [11] N. Tateiwa, Y. Haga, Z. Fisk, and Y. Ōnuki, *Rev. Sci. Instrum.* **82**, 053906 (2011).
  - [12] J. Sugiyama, H. Nozaki, M. Månsson, K. Prša, D. Andreica, A. Amato, M. Isobe, and Y. Ueda, *Phys. Rev. B* **85**, 214407 (2012).
  - [13] S. F. Matar and G. Demazeau, *Chem. Phys. Lett.* **407**, 516 (2005).
  - [14] V. Srivastava, M. Rajagopalan, and S. P. Sanyal, *Eur. Phys. J. B* **61**, 131 (2008).
  - [15] S. Yunoki, J. Hu, A. L. Malvezzi, A. Moreo, N. Furukawa, and E. Dagotto, *Phys. Rev. Lett.* **80**, 845 (1998).
  - [16] E. Dagotto, S. Yunoki, A. L. Malvezzi, A. Moreo, J. Hu, S. Capponi, D. Poilblanc, and N. Furukawa, *Phys. Rev. B* **58**, 6414 (1998).
  - [17] E. Dagotto, T. Hotta, and A. Moreo, *Phys. Rep.* **344**, 1 (2001).
  - [18] Y. Tokura, A. Urushibara, Y. Moritomo, T. Arima, A. Asamitsu, G. Kido, and N. Furukawa, *J. Phys. Soc. Jpn.* **63**, 3931 (1994); A. Urushibara, Y. Moritomo, T. Arima, A. Asamitsu, G. Kido, and Y. Tokura, *Phys. Rev. B* **51**, 14103 (1995).
  - [19] Edited by Anant V. Narlikar, *Frontiers in Superconducting Materials* (Springer, Berlin/Heidelberg/New York, 2005); X. Luo, and X. Chen, *Sci. China. Mater.* **58**, 77 (2015).